Investigation of pulsed laser ablation process of $Hg_{0.8}Cd_{0.2}Te$

Xinling Zhou (周新玲), Chuansong Chen (陈传松), Baoyuan Man (满宝元), and Juan Guo (郭 娟)

College of Physics and Electronics, Shandong Normal University, Ji'nan 250014

Received November 27, 2006

The vaporization threshold was measured under the irradiation of 1.064-μm, 10-ns pulsed laser. Then we calculated the vaporization temperature based on the conservation law of energy and analyzed the vaporization time based on our established model. These results coincided well with the information from the micrograph of scanning electron microscope (SEM) and the spectra of the plasma. Besides, the laser ablation rate was also computed and discussed theoretically.

OCIS codes: 140.0140, 140.3440, 140.6810.

In the interaction between laser and solid target, the interests have been widely concentrated on either the high-density and high-temperature plasmas[1−3] or the generation of shock waves in the unablated material and the resulting high-pressure state[4,5]. Laser ablation, i.e., the ejection and separation of matter out of the laser-heated solid surface, is a basic aspect of laser-matter interaction. Several mechanisms have been proposed, which could be responsible for the laser-induced formation of charged and neutral particles[6−8]. Apart from the basic interest, particular applications would benefit from the improved understanding of ablation process, which generally involves the laser damage of various materials and the laser ablative matter removal for pulsed laser deposition (PLD)[9] and micromachining[10,11].

PLD technique has been extensively employed in preparing thin films of semiconductors[12], as well as superconductors[13]. In comparison with other methods, PLD has many advantages and is a very promising method for growing high quality thin films. Although high quality thin films of superconductor (Y-Ba-Cu-O) have been prepared in many laboratories, preparing high quality thin films of $Hg_{0.8}Cd_{0.2}Te$, one of the important infrared materials, has been being of difficulties. The studies on the melting and plasma of $Hg_{0.8}Cd_{0.2}Te$ have been done by lots of groups[1,14], but the investigation on the laser ablation process of it has been seldom reported. Therefore it is necessary to gain an insight into the laser ablation process of $Hg_{0.8}Cd_{0.2}Te$ at present.

In this paper we measured the vaporization threshold in the case of 1.064-μm and 10-ns pulsed laser irradiating the $Hg_{0.8}Cd_{0.2}Te$ target. The theoretical result is in good agreement with the experimental data. Then the vaporization temperature was calculated numerically based on the energy conservation law and the vaporization time was also analyzed based on our established model[15]. These results were also confirmed by the micrograph of scanning electron microscope (SEM) and the spectra of plasmas. Then, we computed and discussed the laser ablation rate theoretically.

The arrangement of the experimental apparatus has been shown in Ref. [1]. The pulsed laser used in our experiment is a Nd:YAG laser (Spectra Physics Quanta-Ray DCR-3) and operates in a Q-switched mode. The laser output has a pulse duration of 10 ns and a wavelength of 1.064 μm, and the maximum laser energy is 1 J. The laser energy was measured by a digital energy meter (OPHIR DGX-30A). The laser pulse was reflected by a prism mirror, and then focused onto the polished HgCdTe target surface by a quartz focus lens L1 ($f = 6.3$ cm). The focus of the lens was adjusted on the target surface, and the spot size of the laser beam is 0.44 mm in diameter. The HgCdTe sample was positioned on a sample holder in a chamber. The chamber and lens L1 were mounted on a two-dimensional (2D) (x,y directions) movable plates. The y direction is the laser beam axis. In the x direction, two cylindrical lenses (L2 and L3) were used to image the plasma emission from the plane which has a distance d_0 from the surface of the target to the entrance of the slit of a spectrum analyzer (ISA, HR-320). The dispersed emission was subsequently detected with a 10-ns gated, image-intensified optical multichannel analyzer (PARC OMA III). The area irradiated by pulsed laser was scanned and analyzed with a SEM at 20 keV.

In the experiment, we measured the vaporization threshold for six times under 10-ns pulsed laser irradiation. The results were shown in Table 1.

In order to decrease the experimental error, we considered the average data in Table 1 as the vaporization threshold. The average value is 5.5×10^7 W/cm^2 or 0.55 J/cm^2. However, the damage threshold is lower than that measured in Ref. [16] under the 10.6-μm laser irradiation. We thought that there were two reasons could explain the difference. Firstly, since the absorption coefficient of $Hg_{0.8}Cd_{0.2}Te$ crystal for the laser with a wavelength of 1.064 μm (1.0×10^4 cm^{-1}[12,13]) is an order of magnitude more than that for the 10.6-μm laser (1.0×10^3 cm^{-1}[14]), the surface temperature will increase more quickly under 1.064-μm laser irradiation compared

Table 1. Vaporization Threshold for $Hg_{0.8}Cd_{0.2}Te$

Measurement	Threshold Laser Intensity ($\times10^7$ W/cm^2)
1	5.5
2	5.6
3	6.0
4	5.2
5	5.8
6	5.0

1671-7694/2007/080468-04

with under 10.6-μm laser irradiation. Also, the more the absorption coefficient is, the lower the penetration depth gets, and the thinner layer is vaporized. Therefore, the vaporization easily occurs when the 1.064-μm laser instead of 10.6-μm laser is focused on the surface of $Hg_{0.8}Cd_{0.2}Te$ crystal. Secondly, it has been reported that the major response of detector to the irradiation of in-band light is optical effect, while thermal effect can be seen when the incident laser intensity is somewhat higher. However, when irradiated by off-band light, the major response of detector is thermal effect[17]. In our work, the response band of $Hg_{0.8}Cd_{0.2}Te$ is $8-14$ μm, therefore, the thermal effect of 1.064-μm laser pulse outweighs that of 10.6-μm laser pulse.

The vaporization threshold of the pulsed laser could also be computed using the model established in Ref. [14]. The results are shown in Fig. 1. It is evident that the theoretical result, 5.4×10^7 W/cm^2, is very consistent with the experimental data.

In addition, according to the energy conservation law, an expression can be written as

$$E_{\rm th}(1-R)=\rho d\int_{T_0}^{T_{\rm v}}c(T){\rm d}T, \tag{1}$$

where $E_{\rm th}$ is the threshold incident energy density, R the reflectivity, $T_{\rm v}$ and T_0 the vaporization temperature and room temperature, respectively, d the penetration depth $(1/\alpha)$, and $c(T)$ the specific heat. The relation between $c(T)$ and T is given in Ref. [14]. Considering the nonlinear change of $c(T)$ with temperature, the vaporization temperature of 1741 K is obtained by numerical solution.

We also investigated the vaporization time based on the plasma emission spectra[15]. The temporal evolution obtained in the wavelength of $380-620$ nm at an observation distance $d_0=0.5$ mm is shown in Fig. 2. It is obvious that an intense continuous emission spectrum appears at the delay time of 10 ns. Thus we could deduce that the plasma generates within 10 ns after the pulsed laser irradiates the target surface. This is because that the continuum is related to the strong collision between free electrons and excited atoms or ions known as bremsstrahlung, and the recombination of electrons and ions.

In order to further study the vaporization process, we also derived an expression of vaporization time based on the model used in Ref. [15],

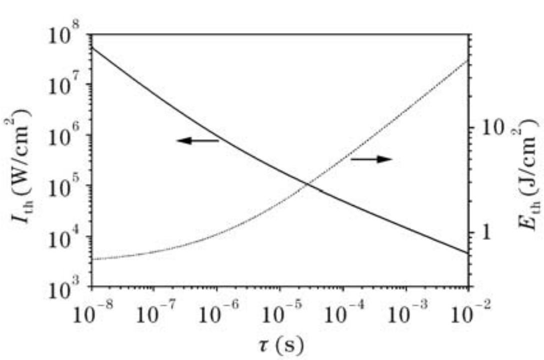

Fig. 1. Time dependence of vaporization threshold for $Hg_{0.8}Cd_{0.2}Te$.

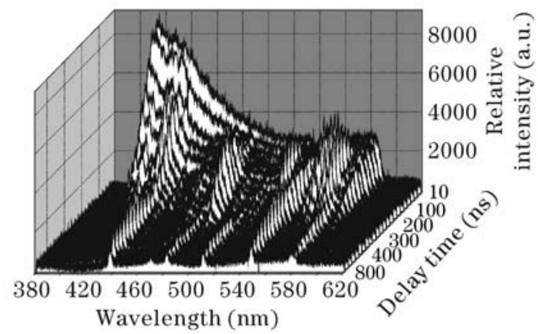

Fig. 2. Evolution of plasma emission spectra in the wavelength region of $380-620$ nm. The corresponding laser intensity is 2.0×10^8 W/cm^2 and the background pressure is 1 atm.

$$t_{\rm v}=\frac{\pi k_{\rm l}\rho_{\rm l}c_{\rm l}(T_{\rm v}-T_{\rm m}+l_{\rm v}/c_{\rm l})}{4[(1-R_{\rm l})I_0]^2}+\frac{\pi k_{\rm s}\rho_{\rm s}c_{\rm s}(T_{\rm m}-T_0+l_{\rm f}/c_{\rm s})}{4[(1-R_{\rm s})I_0]^2}, \tag{2}$$

where $T_{\rm m}$ is the melting point, I_0 the incident laser intensity, $l_{\rm v}$ the vaporization latent, $l_{\rm f}$ the fusion latent, k, ρ, c, and R are thermal conductivity, density, specific heat, and reflectivity, respectively, and the footnotes "l" and "s" denote liquid state and solid state. Using Eq. (2) and the parameters from Ref. [14], we got the results shown in Fig. 3. It reveals that the vaporization time decreases quickly with the increase of incident laser intensity when the laser energy just exceeds the vaporization threshold, and it almost becomes constant when the laser intensity is very high. One could clearly recognize that the vaporization occurs almost instantaneously when the pulsed laser with intensity more than 4.0×10^8 W/cm^2 reaches the target surface. Meanwhile the SEM micrograph shown in Fig. 4 gives that the target surface is already vaporized at the laser power density of 2.0×10^8 W/cm^2 for the sputter phenomenon can be observed apparently.

According to the Beer-Lambert law and pondering on the absorptivity of the target surface and vaporized materials, a relation can be written as

$$I_d=\varepsilon I_0{\rm e}^{-\alpha d}, \tag{3}$$

where ε is the effective absorptivity for incident laser, here considering the absorption of the surface and formed plasma, the average value of ε is taken as 0.22, I_0 and α

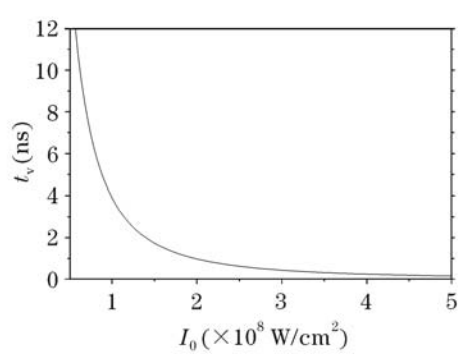

Fig. 3. Vaporization time versus the incident laser intensity.

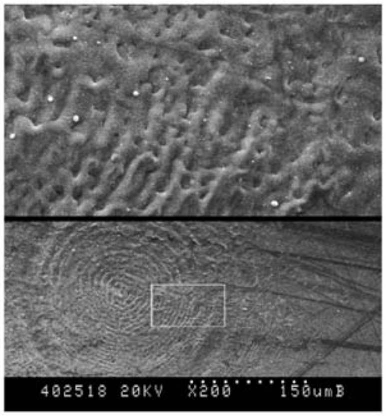

Fig. 4. SEM micrograph of $Hg_{0.8}Cd_{0.2}Te$ surface irradiated by a pulsed laser with the laser intensity of 2.0×10^8 W/cm^2, the magnification of the upper portion is 5 times of the lower.

denote the intensity of the incident laser normal to the surface of target and the absorption coefficient respectively, I_d is the attenuated laser intensity at the depth d into the material. When the laser penetrates the depth d_t, its intensity attenuates to I_th below which no vaporization occurs any longer. Therefore we define the depth d_t as the ablation depth of laser pulse ablation. Solving Eq. (3), we get

$$d_\mathrm{t}=\frac{1}{\alpha}\ln\left(\frac{\varepsilon I_0}{I_\mathrm{th}}\right), \quad (4)$$

where I_th is the power density threshold. So for one pulse the ablation rate can be defined as

$$v_\mathrm{a}=\frac{1}{\alpha}\ln\left(\frac{\varepsilon I_0}{I_\mathrm{th}}\right). \quad (5)$$

It is obvious that the ablation plane moves at a certain velocity, which depends on the properties of the laser and target material, within the laser pulse duration. If the laser irradiates the surface obliquely, the ablation rate should be changed correspondingly as

$$v_\mathrm{a}=\frac{1}{\alpha}\ln\left(\frac{\varepsilon I_0\cos\theta}{I_\mathrm{th}}\right), \quad (6)$$

where θ is the incident angle.

The ablation rate of the pulsed laser irradiation for $Hg_{0.8}Cd_{0.2}Te$ was calculated with Eq. (5) and shown in Fig. 5. From Fig. 5, we can identify two distinct regions. One is that the ablation rate increases rapidly with the increase of the incident laser intensity whose value ranges from the threshold to 1.5×10^9 W/cm^2. This means that if a well stabilized laser with an accurately measurable output is utilized for ablating, this is the desirable region where ablation can be performed most efficiently. However, if the incident laser intensity exceeds 1.5×10^9 W/cm^2, the ablation rate is not very sensitive to it. Therefore, if the laser output is not stable, the appropriate intensity should be selected in the second region for the sake of obtaining a steady ablation rate.

Besides, we computed the variation of the ablation rate with the incident angle. The incident laser intensities were taken as 5.0×10^8, 8.0×10^8, and 1.0×10^9 W/cm^2,

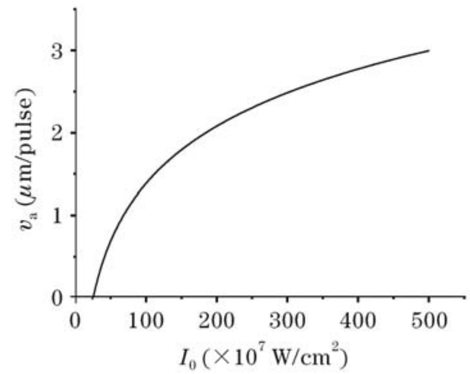

Fig. 5. Incident power density dependence of ablation rate for $Hg_{0.8}Cd_{0.2}Te$.

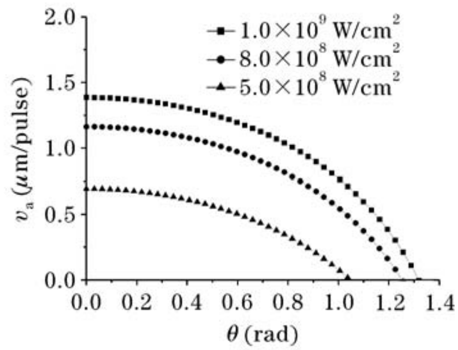

Fig. 6. Incident angle dependence of ablation rate for $Hg_{0.8}Cd_{0.2}Te$.

respectively. The results are shown in Fig. 6. It is evident that when the incident angle is in the range of $0-\pi/4$, the ablation rate is higher and more stable. Therefore, in general we mostly choose the incident angle ranging from 0 to $\pi/4$ in practical applications, such as in PLD. From Figs. 5 and 6, one can easily know that the ablation rate is 1.16 μm/pulse when the pulsed laser with the intensity of 8.0×10^8 W/cm^2 normally irradiates the surface of $Hg_{0.8}Cd_{0.2}Te$ target.

In conclusion, the vaporization threshold of 5.5×10^7 W/cm^2 was measured under the 10-ns pulsed laser irradiation, which agreed well with the calculated result. The vaporization temperature of 1741 K was also computed based on the energy conservation law, and using our established model, one can recognize that the vaporization occurs instantaneously when the laser with the intensity more than 4.0×10^8 W/cm^2 reached the target surface. The ablation rate increased with the increase of the incident laser intensity, and it was about 1.16 μm/pulse at the laser intensity of 8.0×10^8 W/cm^2. The ablation rate was relatively high and stable in the case of the incident angle from 0 to $\pi/4$ at a certain laser intensity. Therefore the laser incident angle should range from 0 to $\pi/4$ in practical applications for high efficiency.

This work was supported by the National Natural Science Foundation of China (No. 10474059), the Provincial Natural Science Foundation of Shandong (No. Y2003A01), and the Project sponsored by SRF for ROCS, SEM, P.R.China. B. Man is the author to whom the correspondence should be addressed, his e-mail address is byman@sdnu.edu.cn.

References

1. B. Y. Man, X. T. Wang, and A. H. Liu, J. Appl. Phys. **83,** 3509 (1998).
2. K. A. Tanaka, R. Kodama., H. Fujita, M. Heya, N. Izumi, Y. Kato, Y. Kitagawa, K. Mima, N. Miyanaga, T. Norimatsu, A. Pukhov, A. Sunahara, K. Takahashi, M. Allen, H. Habara, T. Iwatani, T. Matusita, T. Miyakosi, M. Mori, H. Setoguchi, T. Sonomoto, M. Tanpo, S. Tohyama, H. Azuma, T. Kawasaki, T. Komeno, O. Maekawa, S. Matsuo, T. Shozaki, K. Suzuki, H. Yoshida, T. Yamanaka, Y. Sentoku, F. Weber, T. W. Barbee, Jr., and L. DaSilva, Phys. Plasmas **7,** 2014 (2000).
3. Y. Zhang, C. Chen, X. Zhou, J. Guo, Q. Zhang, and B. Man, Chin. Opt. Lett. **4,** 493 (2006).
4. A. Ng, A. Forsman, and P. Celliers, Phys. Rev. E **51,** R5208 (1995).
5. R. Evans, A. D. Badger, F. Falliès, M. Mahdieh, T. A. Hall, P. Audebert, J.-P. Geindre, J.-C. Gausthier, A. Mysyrowicz, G. Grillon, and A. Antonetti, Phys. Rev. Lett. **77,** 3359 (1996).
6. M. L. Knotek, V. O. Jones, and V. Rehn, Phys. Rev. Lett. **43,** 300 (1979).
7. B. Stritzker, A. Pospieszczyk, and J. A. Tagle, Phys. Rev. Lett. **47,** 356 (1981).
8. T. T. Tsong and T. J. Kinkus, Phys. Rev. B **29,** 529 (1984).
9. G. Kroen, A. Gupta, and R. J. Baseman, Appl. Phys. Lett. **54,** 1920 (1989).
10. V. V. Semak, J. G. Thomas, and B. R. Campbell, J. Phys. D **37,** 2925 (2004).
11. X. Li and X. Zeng, Chin. J. Lasers (in Chinese) **29,** 176 (2002).
12. I. S. Virt, M. Bester, L. Dumanńki, M. Kuźma, I. O. Rudyj, M. S. Frugynskyi, and I. V. Kurilo, Appl. Surf. Sci. **177,** 201 (2001).
13. G. Kroen, A. Gupta, R. J. Baseman, M. L. Lutwyche, and R. B. Laibowitz, Appl. Phys. Lett. **55,** 2450 (1989).
14. M. M. Jevtić and M. J. Šćepanović, Appl. Phys. A **53,** 332 (1991).
15. C. S. Chen, A. H. Liu, G. Sun, J. L. He, X. Q. Wei, M. Liu, Z. G. Zhang, and B. Y. Man, J. Opt. A **8,** 88 (2006).
16. F. Bartoli, L. Esterowitz, M. Kruer, and R. Allen, J. Appl. Phys. **46,** 4519 (1975).
17. X. Li, X. Cheng, R. Wang, L. Ma, and Q. Lu, Chin. J. Lasers (in Chinese) **30,** 1070 (2003).